Supplementary information for

Oxygen Regulation of Breathing is Abolished in Mitochondrial Complex III-Deficient Arterial Chemoreceptors

Daniel Cabello-Rivera[1,2,3#], Patricia Ortega-Sáenz[1,2,3#*], Lin Gao[1,2,3], Ana M. Muñoz-Cabello[1,2,3], Victoria Bonilla-Henao[1,2,3], Paul T. Schumacker[4], and José López-Barneo[1,2,3*]

***To whom correspondence should be addressed:**
Instituto de Biomedicina de Sevilla (IBiS), Campus Hospital Universitario Virgen del Rocío, Avenida Manuel Siurot s/n 41013 Seville, Spain
Phone: +34 955 923032
Email: lbarneo@us.es
Email: gortega1@us.es

This PDF file includes:
Materials and Methods
Figures S1 to S4
SI References

Materials and Methods

Mouse genotyping

The genotype of each mouse was determined by PCR using the following primers: 5'-CTTGAACTTGAGAAAAGGTGGGGA-3' and 5'-CCAACTAAGTGGTTTTGCACAGGG-3' for Uqcrfs1; 5'-CACCCTGACCCAAGCACT-3', 5'-CTTTCCTTCCTTTATTGAGAT-3', 5'-GATACCTGGCCTGGTCTG-3' for Cre.

Measurement of hematocrit and growth hormone

To measure hematocrit, blood was collected from an incision in the heart using a hematocrit tube located near the incision site. After blood filled by capillarity the hematocrit tube, the ends of the tube were sealed with bone wax and the tubes placed in a microhematocrit centrifuge and centrifuged for 5 minutes at high speed. The length of the column of packed red cells and total blood length were measured and the hematocrit expressed as the percentage of erythrocytes relative to total blood volume. Growth hormone (GH) content in serum was determined using an ELISA kit (Millipore) following manufacturer's instruction. In brief, whole blood was collected into a centrifuge tube without anticoagulant. Following clot formation, serum was separated from the clotted blood by centrifugation at 3000 g for 15 min at 4°C. Serum samples were aliquoted and stored at -80°C until the measurement. 10 µl of each serum sample were used to measure GH content.

Preparation of carotid body slices and dispersed glomus cells

CB slices were used to measure secretory activity by amperometry and ROS production by microfluorimetry. Dissected carotid bodies were included in 1% (w/v) low melting point agarose in PBS (42ºC). Mice CB sections (150 µm thick) were cut with a vibratome (VT1000S, Leyca) in cold PBS solution and slightly digested with an enzymatic solution (PBS pH 7.4 supplemented with 50 µM $CaCl_2$, 0.6 mg/ml collagenase II (Sigma), 0.27 mg/ml trypsin (Sigma) and 1.25 U/ml porcine elastase (Calbiochem)) for 5 min at 37°C. Finally, slices were washed twice with PBS and cultured at 37°C in a 5% CO_2 incubator in DMEM (0 glucose)/DMEM-F12 (GIBCO) medium (3:1) supplemented with 100 U/ml penicillin (Bio-Witthaker), 10 mg/ml streptomycin (Bio-Witthaker), 2 mM L-glutamine (BioWhittaker), 10% fetal bovine

serum (Gibco), 84 U/L insulin (Actrapid), and 1.2 U/ml erythropoietin. Slices were used after 24-48h of incubation. Further details of CB slicing and culture can be found in methodological papers of our laboratory (1,2). For enzymatic CB glomus cell dispersion CBs were incubated for 20 min at 37°C in an enzymatic solution prepared in PBS containing: 50 µM $CaCl_2$, collagenase type II (0.6 mg/ml), trypsin (0.3 mg/ml) and porcine elastase (1.25 U/ml). Thereafter, the CB tissue was teased apart with forceps and incubated for 5 min at 37°C in the same solution. Finally, cells were mechanically dispersed using a pipette and centrifuged for 5 min at 300 g. The cell pellet was resuspended in the same culture medium used for the CB slices and plated on glass cover slips treated with poly-L-lysine. Dispersed cells were maintained at 37°C in a 5% CO_2 and 21% O_2 incubator and used after 24h of incubation. Further details of mouse CB cell dispersion are given in a previous methodological publication of our laboratory (3).

Immunohistochemistry

For immunofluorescent studies, mice were first perfused with PBS and then with 4% paraformaldehyde in PBS before tissue dissection. The dissected carotid bifurcation was fixed with 4% paraformaldehyde in PBS for 2 hours, cryoprotected overnight with 30% sucrose in PBS, and embedded in OCT (Tissue-Tek). Tissue sections of 10 µm were cut with a cryostat (Leica). Tissue sections were incubated with primary antibodies against TH (1:1000 dilution, NB300-109, Novus Biological Inc. or 1:200 dilution, AB1542, Millipore) and NDUFA4L2 (1:50 dilution, 16480-1-AP, Proteintech) overnight at 4°C. This was followed by incubation with fluorescent secondary antibodies Alexa Fluor 568 (1:500 dilution, A11011, Invitrogen) and Alexa Fluor 488 (1:500 dilution, A11008 or A11015, Invitrogen). Nuclei were labeled with 4′,6′-diamidino-2-phenylindole (DAPI). Immunofluorescent images were obtained using an Olympus BX61 microscope. Confocal images were acquired with a Leica Stellaris 8 confocal microscope. Photographs of immunostained tissues were analyzed with ImageJ software to blindly quantify the volume of SCG and the number of TH-positive cells in the CB. Mouse brains were fixed overnight with 4% paraformaldehyde in PBS and paraffin-embedded. Coronal sections 20 µm-thick were cut with a microtome (Leica). Immunoreactivity against TH antibody (1:2500 dilution, NB300-109, Novus Biological Inc.) was detected with 3,3-diaminobenzidine

(DAB) using Envision$^+$ System-HRP (Dako Cytomation) according to the manufacturer's instructions. Immunochemical images were obtained using an Olympus BX61 microscope.

Amperometry

To record quantal exocytotic release of catecholamines from glomus cells in CB slices we used the amperometry technique. For each experiment, a CB slice was transferred to the recording chamber and perfused continuously with recording solutions bubbled with different gas mixtures (see "Recording solutions" in main text). Secretory events were recorded with a polarized (+750 mV) carbon fiber electrode (10 µm diameter) mounted on a micromanipulator and placed near the glomus cell under microscope control (upright Axioscope, Zeiss). Amperometric currents were recorded with an EPC-7 patch-clamp amplifier (HEKA Electronics). Data acquisition and analysis were carried out with an ITC-16 interface (Instrutech Corporation) and PULSE/PULSEFIT software (HEKA Electronics). The secretion rate (fC or pC/min) was calculated as the amount of charge transferred to the recording electrode during the last minute of exposure to the stimulus. Basal secretion rate was calculated during a minute in normoxia. Cumulative secretion was calculated as the time integral of the amperometric recording. Further details are given in methodological publications of our laboratory (1,4).

Microfluorimetry

To perform cytosolic Ca^{2+} measurements, CB dispersed cells were incubated in DMEM/F-12 (without FBS) containing 2 µM Fura 2-AM (F-1221, Molecular Probes) for 20 minutes at 37°C in a 5% CO_2 incubator. After washing with complete culture medium for 10 min, the coverslip with Fura 2-AM loaded cells was placed on the recording chamber mounted on the stage of an inverted microscope (Nikon eclipse Ti) equipped with a 40x/0.60 NA objective, a monochromator (Polychrome V, Till Photonics), and a CCD camera, controlled by Aquacosmos software (Hamamatsu Photonics). 340 and 380 nm alternating wavelength were used to excite FURA-2 and an emission wavelength of 510 nm were used to obtain the F340/F380 ratio (5). Cytosolic Ca^{2+} signals were digitized at a sampling interval of 500 ms. The acquisition protocol was designed with a spatial resolution of 4x4 pixels, an excitation

time of 20 ms and an acquisition interval of 5 s. A dichroic FF409-Di03 (Semrock) and a band pass filter FF01-510/84 (Semrock) were used.

NAD(P)H microfluorimetric measurements were performed in CB dispersed cells using a non-ratiometric protocol taking advantage of the NAD(P)H autofluorescence and using the same set up described for cytosolic Ca^{2+} measurements. NAD(P)H was excited at 360 nm and measured at 460 nm. Although the UV-excited NAD(P)H autofluorescence signals mostly report on the mitochondrial NAD(P)H pool (6-8), it seems that in glomus cells the activity of NADH shuttles rapidly equilibrates mitochondrial NADH with the cytosolic pool. In these cells, hypoxia-induced NADH autofluorescence is rapidly inhibited by extracellular application of alpha-ketobutyrate (αKB), which after been transported through the membrane consumes NADH to synthesize alpha-hydroxybutyrate in the cytosol (9). Moreover, hypoxia-induced secretion in glomus cells was rapidly inhibited by extracellular application of αKB (see Fig. 4G in main text). The acquisition protocol was designed with a spatial resolution of 4x4 pixels, an excitation time of 150 ms and an acquisition interval of 5 s. Background fluorescence was subtracted in all experiments.

Recordings of rapid changes in ROS production were performed in glomus cells in CB slices, using a redox-sensitive, green fluorescent protein (roGFP) probe targeted to either the mitochondrial intermembrane space (IMS) or mitochondrial matrix (9,10). This probe is insensitive, or minimally sensitive, to pH (10,11), however it has been reported before that intracellular pH in glomus cells is unaltered by hypoxia (12). To infect CB cells with the adenoviral vector (ViraQuest Inc), freshly prepared slices were incubated in complete culture medium supplemented with $5.5x10^8$ particles/ml IMS-roGFP (VQAd CMV GDP-roGFP), or $6x10^8$ particles/ml matrix-roGFP (VQAd CMV mito-roGFP) to target to specific subcellular compartments. After 48h of incubation, infected CB slice expressing roGFP, was transferred to the recording chamber and superfused with the external solution (see "Recording solutions" in the main text). A dichroic Di02-R488 (Semrock) and a band pass filter FF01-520/35 (Semrock) were used for the experiments. RoGFPs was excited at 400 and 484 nm, and emission recorded at 535 nm, allowing ratiometric measurements of rapid and reversible changes in cellular redox state. To ensure that the probe was working correctly, slices were exposed to 0.2 mM H_2O_2 to measure

rapid cell maximum oxidation. The acquisition protocol was designed with a spatial resolution of 8x8 pixels, an excitation time of 20 ms and an acquisition interval of 5 s. Background fluorescence was subtracted in all the experiments. Further details of this experimental protocol are given in a previous methodological publication of our laboratory (2).

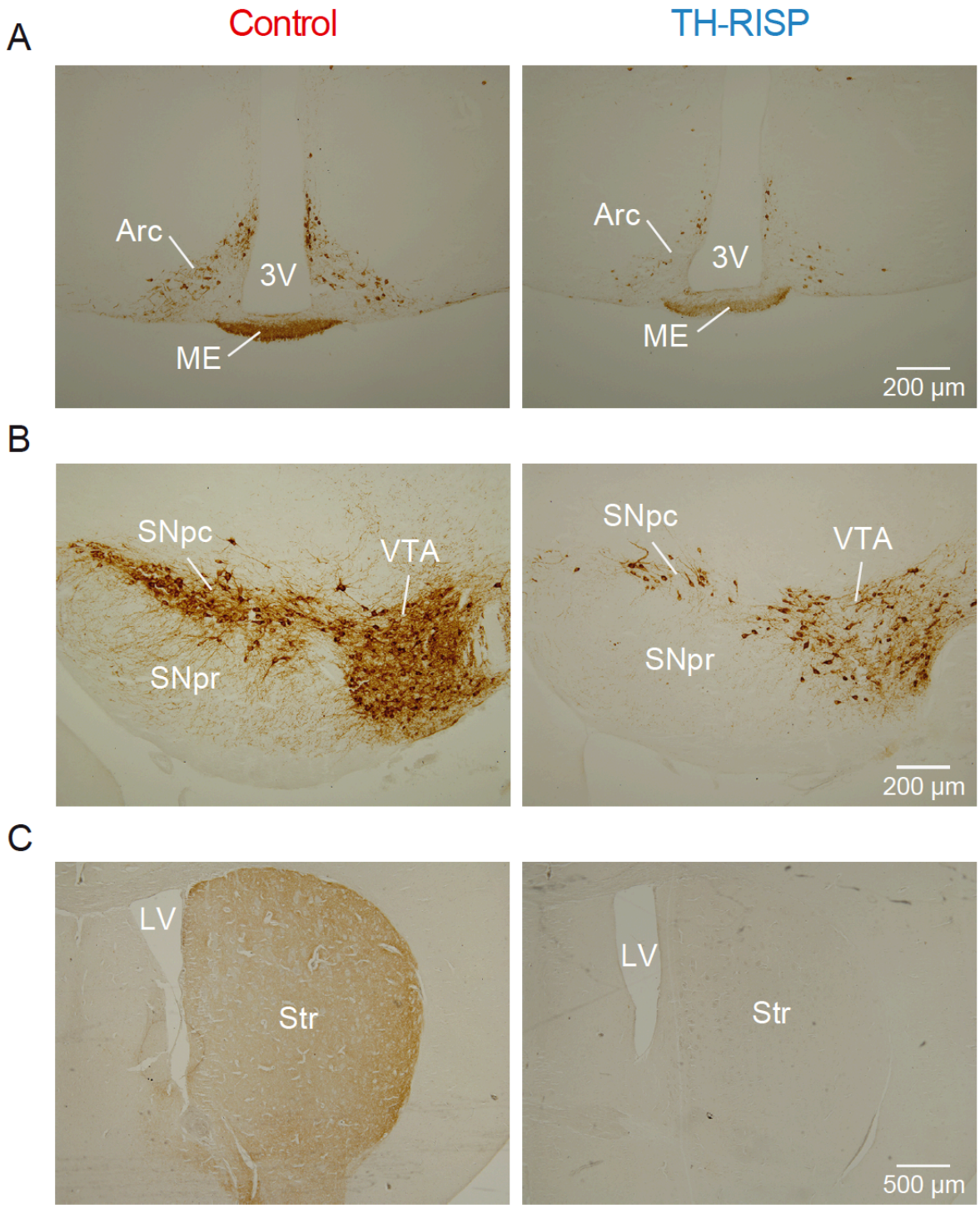

Figure S1. Loss of central catecholaminergic (TH^+) neuronal phenotype in TH-RISP mice. *(A-C)* Representative coronal brain sections of the basal hypothalamus *(A),* mesencephalon *(B),* and basal ganglia *(C)* from control and TH-RISP mice (~P40) immunostained with tyrosine hydroxylase (TH) antibody. Arc, arcuate nucleus; ME, median eminence; 3V, third ventricle; SNpc, substantia nigra *pars compacta*; SNpr, substantia nigra *pars reticulata*; VTA, ventral tegmental area; LV, lateral ventricle; Str, striatum.

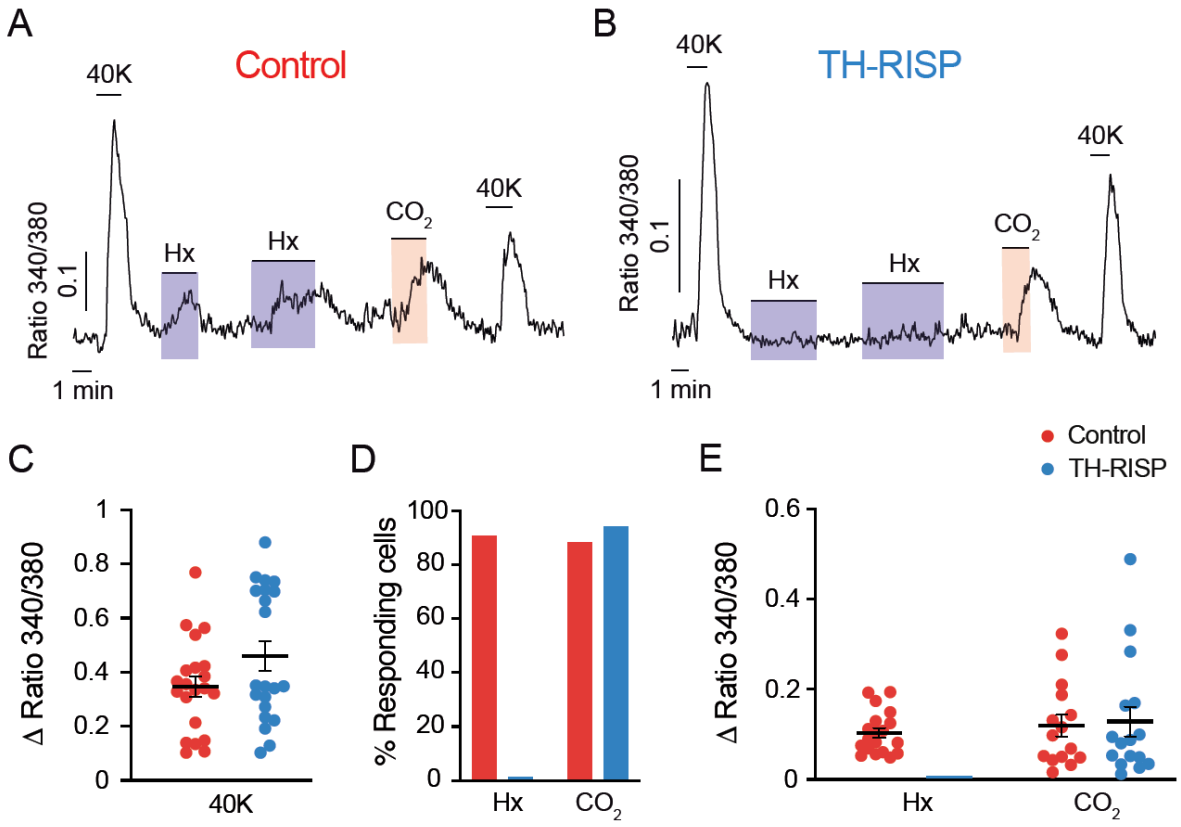

Figure S2. Selective abolition of the hypoxia-induced increase in cytosolic Ca^{2+} in dispersed RISP-deficient glomus cells. *(A,B)* Representative recordings of the increases in cytosolic [Ca^{2+}] elicited by hypoxia (Hx), hypercapnia (CO_2) and high K^+ (40K) in Fura2-loaded glomus cells from control *(A)* and TH-RISP *(B)* mice. *(C)* Average increase in cytosolic [Ca^{2+}] in response to depolarization with 40 mM K in control (0.35±0.04, n= 21 cells/7 mice) and RISP-deficient (0.46±0.05, n=21 cells/9 mice) cells. *(D)* Percentage of control and RISP-deficient cells with an increase in cytosolic [Ca^{2+}] in response to hypoxia (Hx, ~15 mm Hg O_2) and hypercapnia (20% CO_2) Number of cells recorded were: control hypoxia control (21 cells/7 mice); hypoxia RISP-deficient hypoxia (21 cells/9 mice); hypercapnia control (17 cell/7 mice); hypercapnia RISP-deficient (17 cells/9 mice). *(E)* Quantification of the increase in cytosolic [Ca^{2+}] induced by hypoxia (control: 0.104±0.011, n=19 cells/7 mice; RISP-deficient: 0 cells responded) and hypercapnia (control: 0.120±0.024, n=15 cells/7 mice; RISP-deficient: 0.129±0.033; n=16 cells/9 mice). Data are expressed as mean±SEM. Unpaired Student's *t*-test.

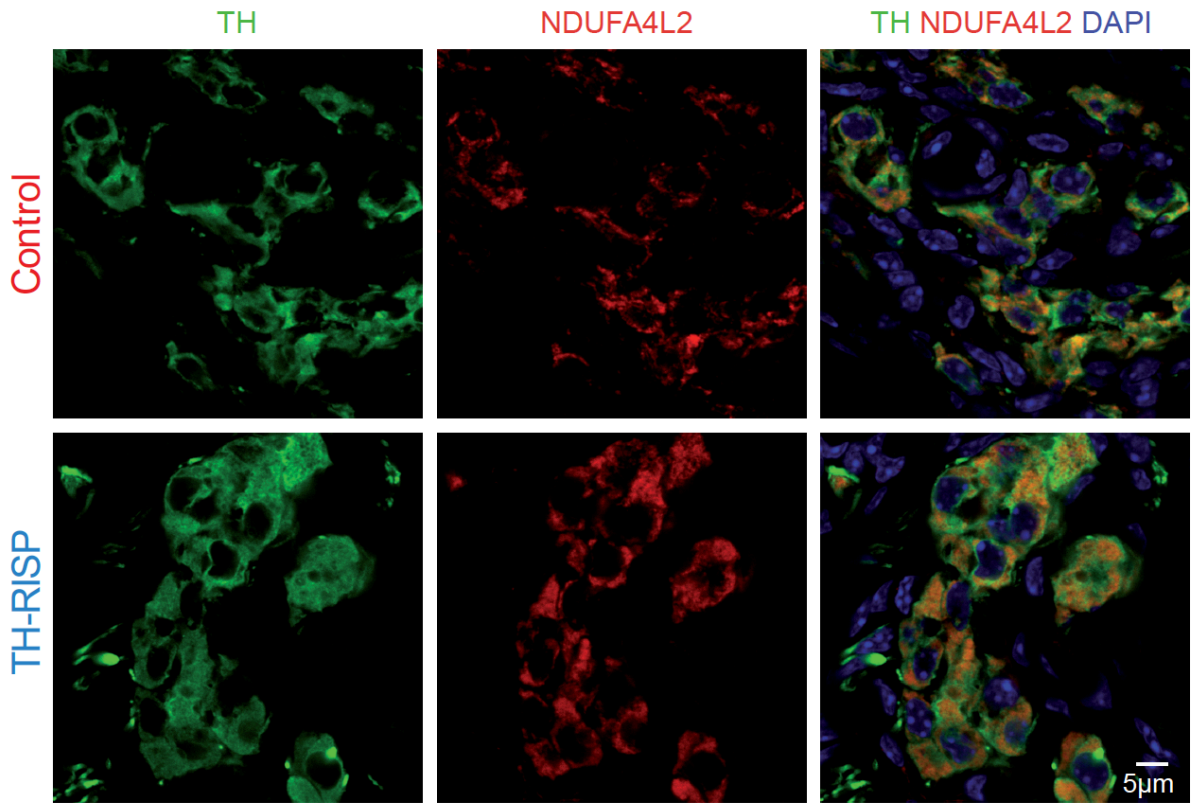

Figure S3. Immunocytochemical localization of mitochondria in control and TH-RISP glomus cells. Glomus cells were stained with antibodies against tyrosine hydroxylase (TH). Antibodies against NDUFA4L2 (a protein highly expressed in glomus cell mitochondria [ref. 13]) were used to stain mitochondria. Representative photographs of additional similar experiments performed in n=6 mice. Nuclei were counterstained with DAPI (blue). Note that the area of mitochondria in TH-RISP cells was similar or even larger than in control cells.

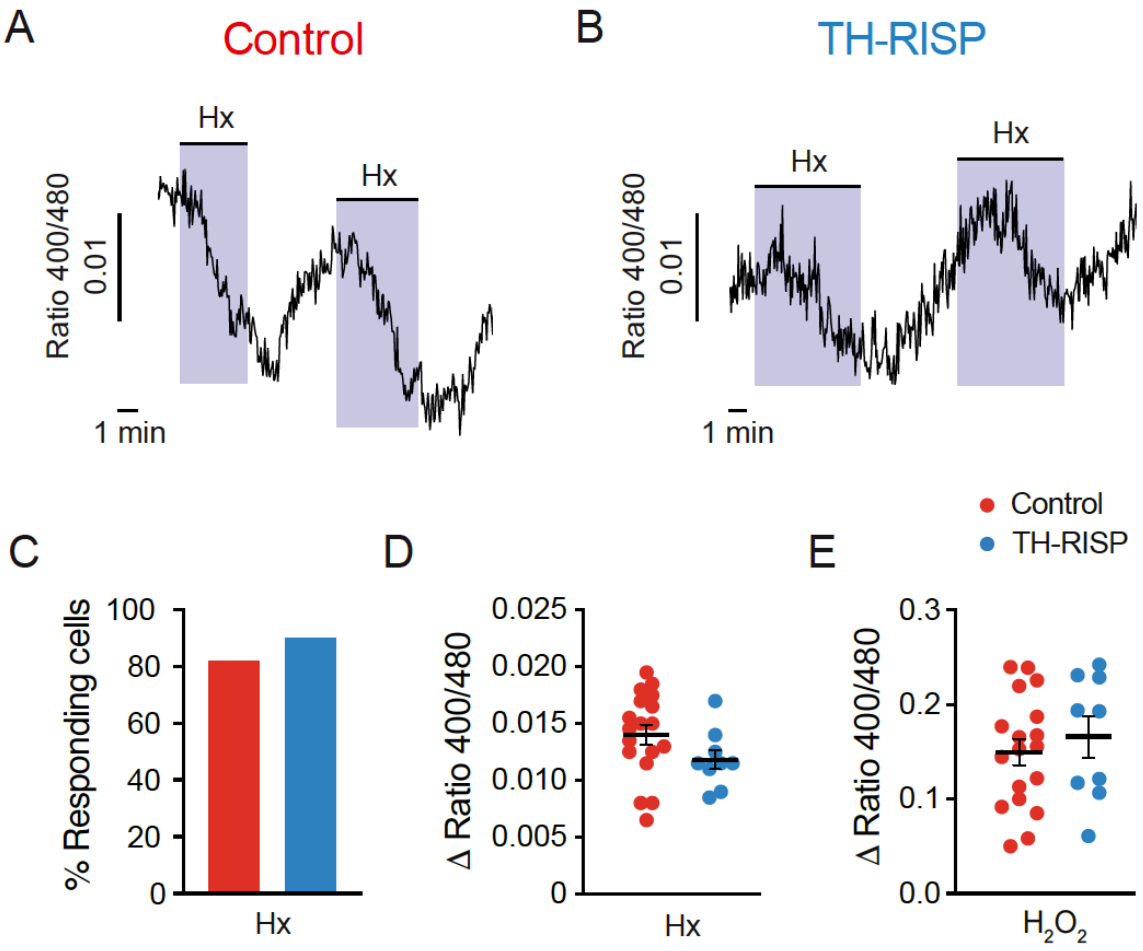

Figure S4. Changes in matrix ROS during hypoxia are conserved in RISP-deficient glomus cells. *(A,B)* Representative recordings of the reversible decrease in matrix ROS induced by hypoxia (Hx, O_2 tension ~15 mm Hg) in glomus cells from control *(A)* and TH-RISP (*B)* mice. *(C)* Percentage of cells with a decrease in matrix ROS during hypoxia (control: n=22 cells tested/14 mice; TH-RISP: n=10 cells tested/6 mice). *(D)* Quantification of the decrease in matrix ROS during exposure to hypoxia in glomus cells from control (0.014±0.001, n=18 cells/10 mice) and TH-RISP (0.012±0.001, n=9 cells/5 mice) mice. (*E*) Increase in matrix ROS (Δ 400/480 ratio) in response to 0.2 mM H_2O_2 in control (0.150±0.014, n=18 cells/9 mice) and RISP-deficient (0.166±0.022, n=9 cells/5 mice) glomus cells. Data are expressed as mean±SEM. Unpaired Student's *t*-test.

References

1. P. Ortega-Saenz, C. Caballero, L. Gao, J. Lopez-Barneo. Testing acute oxygen sensing in genetically modified mice: Plethysmography and amperometry. *Methods Mol Biol* **1742**,139-153 (2018).

2. L. Gao, I. Arias-Mayenco, P. Ortega-Saenz, J. Lopez-Barneo. Using redox-sensitive fluorescent probes to record real-time reactive oxygen species production in cells from mouse carotid body slices. *STAR Protoc* **2,**100535 (2021).

3. A. M. Munoz-Cabello, H. Torres-Torrelo, I. Arias-Mayenco, P. Ortega-Saenz, J. Lopez-Barneo. Monitoring functional responses to hypoxia in single carotid body cells. *Methods Mol Biol* **1742**,125-137 (2018).

4. P. Ortega-Saenz, K. L. Levitsky, M. T. Marcos-Almaraz, V. Bonilla-Henao, A: Pascual, J. Lopez-Barneo. Carotid body chemosensory responses in mice deficient of TASK channels. *J Gen Physiol* **135**, 379-392 (2010).

5. Urena J, Fernandez-Chacon R, Benot AR, Alvarez de Toledo GA, Lopez-Barneo J. Hypoxia induces voltage-dependent Ca2+ entry and quantal dopamine secretion in carotid body glomus cells. *Proc Natl Acad Sci U S A* **91**, 10208-10211 (1994).

6. M. Duchen. Ca^{2+}-dependent changes in the mitochondrial energetics in single dissociated mouse sensory neurons. *Biochem J* **283**, 41-50 (1992).

7. A. M. Brennan, J. A. Connor, C. W. Shuttleworth. NAD(P)H fluorescence transients after synaptic activity in brain slices: predominant role of mitochondrial function. *J Cereb Blood Flow Metab* **26**, 1389-1406 (2006).

8. C. M. Diaz-Garcia, D. J. Meyer, N. Nathwani, M. Rahman, J. R. Martinez-Francois, G. Yellen. The distinct roles of calcium in rapid control of neuronal glycolysis and the tricarboxylic acid cycle. *Elife* **10**, e64821 (2021).

9. I. Arias-Mayenco et al. Acute O_2 sensing: Role of coenzyme QH_2/Q ratio and mitochondrial ROS compartmentalization. *Cell Metab* **28**,145-158 (2018).

10. G. B. Waypa et al. Hypoxia triggers subcellular compartmental redox signaling in vascular smooth muscle cells. *Circ Res* **106**, 526-535 (2010).

11. G. T: Hanson, R. Ahheler, D. Oglesbee, M. Cannon, R. A. Capaldi, R. Y. Tsien, S. J. Remington. Investigating mitochondrial redox potential with redox-sensitive green fluorescent protein indicators. *J Biol Chem* **279**, 13044-13053 (2004).

12. A. Mokashi, D. Ray, F. Botre, M. Katayama, S. Osanai, S. Lahiri. Effect of hypoxia on intracellular pH of glomus cells cultured from cat and rat carotid bodies. *J Appl Physiol (1985)* **78**, 1875-1881 (1995).
13. A. Moreno-Dominguez *et al.*, Acute O_2 sensing through HIF2alpha-dependent expression of atypical cytochrome oxidase subunits in arterial chemoreceptors. *Sci Signal* **13,** eaay9452 (2020).